AD_____

Award Number: W81XWH-10-1-0669

TITLE: UV-Induced Triggering of a Biomechanical Initiation Switch Within Collagen Promotes Development of a Melanoma-Permissive Microenvironment in the skin

PRINCIPAL INVESTIGATOR: Peter Brooks, Ph.D.

CONTRACTING ORGANIZATION: Maine Medical Center, Portland, ME 04102-3134

REPORT DATE: September 2012

TYPE OF REPORT: Annual

PREPARED FOR: U.S. Army Medical Research and Materiel Command
Fort Detrick, Maryland 21702-5012

REPORT DOCUMENTATION PAGE

Form Approved
OMB No. 0704-0188

1. REPORT DATE	2. REPORT TYPE	3. DATES COVERED
01-09-2012	Annual	1 SEP 2011 - 31 AUG 2012

4. TITLE AND SUBTITLE
UV Induced Triggering of a Biomechanical Initiation Switch Within Collagen Promotes Development of a Melanoma-Permissive Microenvironment in the Skin

5a. CONTRACT NUMBER

5b. GRANT NUMBER
W81XWH-10-1-0669

5c. PROGRAM ELEMENT NUMBER

6. AUTHOR(S) **Peter Brooks, Ph.D.**

E-Mail: brookp1@mmc.org

5d. PROJECT NUMBER

5e. TASK NUMBER

5f. WORK UNIT NUMBER

7. PERFORMING ORGANIZATION NAME(S) AND ADDRESS(ES)

Maine Medical Center

Portland, ME 04102-3134

8. PERFORMING ORGANIZATION REPORT NUMBER

9. SPONSORING / MONITORING AGENCY NAME(S) AND ADDRESS(ES)
U.S. Army Medical Research and Materiel Command
Fort Detrick, Maryland 21702-5012

10. SPONSOR/MONITOR'S ACRONYM(S)

11. SPONSOR/MONITOR'S REPORT NUMBER(S)

12. DISTRIBUTION / AVAILABILITY STATEMENT
Approved for Public Release; Distribution Unlimited

13. SUPPLEMENTARY NOTES

14. ABSTRACT
The overall objective of our proposal was to test whether UV irradiation facilitates the exposure of the HU177 cryptic collagen epitope which may represent an early "solid state biomechanical initiation switch" that promotes inflammation, skin damage and the creation of a melanoma permissive niche. Our current studies suggest that UV-mediated structural alterations in collagen type-I, collagen type-IV and Matrigel™ differentially alter the ability of human melanoma cells, human dermal fibroblasts and macrophages to attach, migrate and proliferate on these ECM substrates. These in vitro results are consistent with the possible ability of UV-irradiation of ECM proteins to differentially alter the response of distinct subsets of tumor and normal stromal cells to ECM proteins that help compose the skin microenvironment. In addition, our new data suggest that pre-treating mice with anti-HU177 antibody inhibited UVB-induced accumulation of mast cells in the skin. Moreover, pre-treating mice with a single dose of anti-HU177 antibody also reduced the UV-associated increase in tumor growth by nearly 40%. Taken together, these new data suggest a functional role the HU177 collagen epitope in UV-enhanced inflammation and tumor growth in vivo.

15. SUBJECT TERMS
Biomechanical switch -- Collagen structure -- Conformational change -- Cell adhesion -- Melanoma cells – Fibroblast-- Macrophages

16. SECURITY CLASSIFICATION OF:			17. LIMITATION OF ABSTRACT	18. NUMBER OF PAGES	19a. NAME OF RESPONSIBLE PERSON
a. REPORT	b. ABSTRACT	c. THIS PAGE			USAMRMC
U	U	U	UU	18	19b. TELEPHONE NUMBER *(include area code)*

Table of Contents

Introduction: The overall objective of our proposal was to test whether UV irradiation facilitates the exposure of the HU177 cryptic collagen epitope which may represent an early "solid state biomechanical initiation switch" that promotes inflammation, skin damage and the creation of a melanoma permissive niche. In this regard, we have proposed to assess whether selective targeting of this biomechanical initiation switch prevents or reduces UV-induced inflammation and to examine whether it represents a novel therapeutic approach to prevent and/or reduce melanoma growth. First, we will characterize the kinetics of UV-induced exposure of the HU177 cryptic epitope in vitro and in vivo. These studies will be carried out using a combination of in vitro biochemical assays, ELISAs and immunohistochemical analysis of UV irradiated-collagen as well as the basement membrane preparation Matrigel^{TM}. In the second aim, we will evaluate the impact of UV-induced biomechanical alterations in collagen and the basement membrane preparation Matrigel^{TM} has on inflammatory cell, dermal fibroblast, and melanoma cell adhesion, migration, invasion and proliferation as compared to non UV-irradiated ECM. Finally, we will determine the biological consequences of UV-induced exposure of the HU177 cryptic epitope has on inflammatory cell infiltration and on the ability of melanoma cells to establish tumors in vivo.

Body: We have made considerable progress towards the goals of our proposal during the second funding period (September 2011 through September 2012). In particular, we have made substantial progress on all specific aims (1-3) and their associated tasks. A detailed summary of the research accomplishments as they pertain to the tasks outlined in the statement of work is provided below. Our previous studies have indicated that UVA and UVB irradiation can dose dependently trigger conformational changes in both collagen type-I and collagen type-IV resulting in the exposure of the HU177 cryptic collagen epitope. Importantly, the relative levels of exposure of the HU177 epitope as indicated by ELISA varied depending on the collagen type, wavelength and dose of UV irradiation. In addition, our previous studies indicated that melanoma cell adhesion was generally enhanced on UV irradiated collagen. Importantly, to rule out a possible role for thermal denaturation as a result of UV-irradiation in the exposure of the HU177 epitope, we examined the temperature during UV-irradiation at all doses used. Our studies indicate only a small change in temperature from 20.5^0C to 22.2^0C. These data suggest that the exposure of the HU177 epitope detected in vitro following UV-irradiation was unlikely do to thermal denaturation. Interestingly, macrophage adhesion to UVB irradiated collagen type-IV but not type-I was dramatically enhanced, suggesting a complex cell type and collagen specific response to distinct UV wavebands in vitro. These novel findings are consistent with the possibility that unique physical alterations in the three-dimensional structure of ECM proteins may represent a mechanism to initiate triggering of a biomechanical switch that allows multiple cell types within the tissue microenvironment to differentially interact with cryptic epitopes thereby altering their behavior. These differential interactions may play a role in governing inflammation and melanoma tumor initiation and progression.

Summary of research accomplishments

UVA-irradiation of collagen type-I alters human M21 melanoma and fibroblast adhesion. Our previous studies suggested that structural changes induced by UVB-irradiation (310nm) of collagen type-IV, but not collagen type-I could differentially impact cell adhesive behavior in vitro. To examine whether the longer wavelength UVA (365nm) could alter behavior of human melanoma cells and human dermal fibroblasts, cell adhesion assays were carried out with collagen type-I that was not irradiated or irradiated with UVA over a dose range (0 to 5.0J/cm^2). As shown in figure 1A, M21 melanoma cells exhibited an approximately 50% increase in their ability to adhere to collagen type-I irradiated with UVA at a dose of 5.0J/cm^2, while little impact was observed at lower doses. The ability of fibroblast to attach to UVA irradiated collagen type-I was only marginally enhanced (figure 1B). These data are consistent with our previous studies indicating a dose and cell type specific alteration in cell adhesive behavior following UV irradiation.

A. **B.**

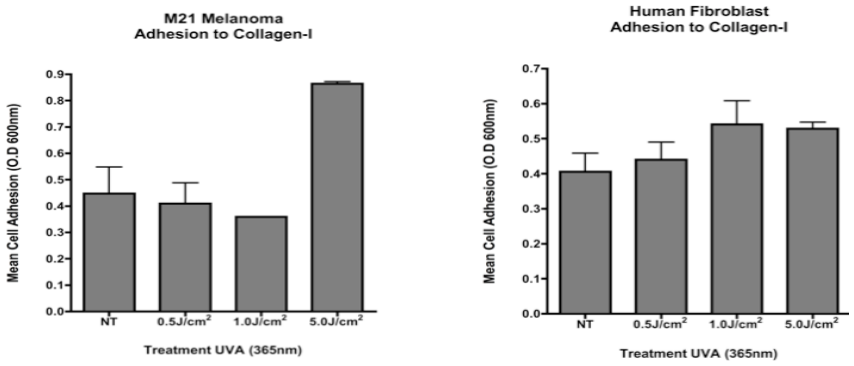

Figure 1. Alteration of cell interactions with UVA-irradiated collagen type-I. Non-treated and irradiated collagen type-I were coated (5.0ug/ml) on wells and blocked with BSA. A). M21 melanoma cells or B) human dermal fibroblasts were seeded on the wells and allowed to attach as we described (1-3). Data bars represent mean cell adhesion (Optical Density O.D) ± standard deviations from triplicate wells.

UVA-irradiation of collagen type-IV differentially alters human M21 melanoma and fibroblast adhesion. Given our studies suggesting UVA irradiation of collagen type-I may alter cell adhesion, we carried out similar studies using basement membrane collagen type-IV. As shown in figure 2A, a small increase in M21 melanoma cell adhesion to UVA-irradiated collagen type-IV at a dose of 0.5 and 1.0J/cm^2, while little impact was observed at 5.0J/cm^2. The ability of fibroblasts to attach to UVA irradiated collagen type-IV was also marginally enhanced at 5.0J/cm^2 (figure 2B).

A. **B.**

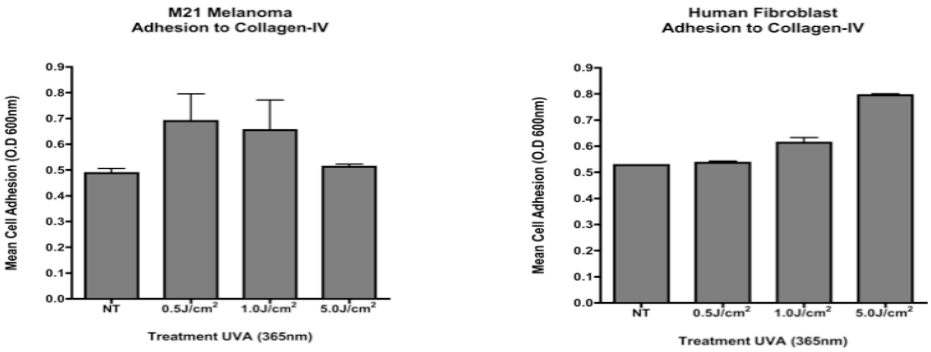

Figure 2. Alteration of cell interaction with UVA-irradiated collagen type-IV. Non-treated and irradiated collagen type-IV were coated (5.0ug/ml) on wells and blocked with BSA. A). M21 melanoma cells or B) human dermal fibroblasts were seeded on the wells and allowed to attach as we described (1-3). Data bars represent mean cell adhesion (Optical Density O.D) ± standard deviations from triplicate wells.

UVA-irradiation of collagen type-I differentially alters human melanoma and fibroblast proliferation in vitro. To assess the effects of UVA irradiation of collagen type-I on melanoma and fibroblast cell growth in vitro, we carried out in vitro proliferation assays. Briefly, interstitial collagen type-I was either untreated or irradiated with UVA over a dose range (0-5.0 J/cm^2) and proliferation was assessed over a time course (0-72hrs). Little change in the proliferation of either M21 melanoma or fibroblasts was observed under the experimental conditions within the first 48hrs. However, as shown in figure 3A, a small reduction was observed in M21 melanoma cell growth on UVA (0.5J/cm^2) irradiated collagen by day 3. In contrast, an approximately 50% increase in fibroblast cell growth was observed by day 3 on UVA irradiated collagen type-I at a dose of 0.5J/cm^2 or higher (figure 3B).

A. **B.**

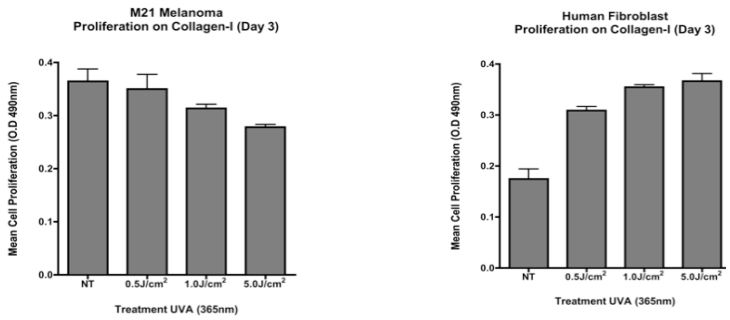

Figure 3. UVA-irradiation of collagen type-I alters melanoma and fibroblast growth in vitro. Collagen type-I was not treated or irradiated with UVA (365nm) over a dose range (0-5.0J/cm^2). Wells were coated (5.0ug/ml) with untreated or UVA treated collagen and M21 melanoma cells (A) or human dermal fibroblasts (B) were seeded and allowed to grow over a 3-day time course. Proliferation was monitored using MTT assay. Data bars represent mean proliferation (Optical Density O.D) ± standard deviations from triplicate wells on Day 3.

UVA-irradiation of collagen type-IV alters human melanoma and fibroblast proliferation in vitro. To assess the effects of UVA irradiation of collagen type-IV on melanoma and fibroblast cell growth in vitro, we carried out proliferation assays essentially as described above. Again, little change in the proliferation of either M21 melanoma or fibroblasts was observed within the first 48hrs. However, as shown in figure 4A, similar to what was observed on collagen type-I, a small reduction was observed in M21 melanoma cell growth on UVA irradiated collagen as compared to control and an approximately 38% increase in fibroblast cell growth was observed by day 3 on UVA irradiated collagen at a dose of 0.5J/cm^2 or higher (figure 4B).

A. **B.**

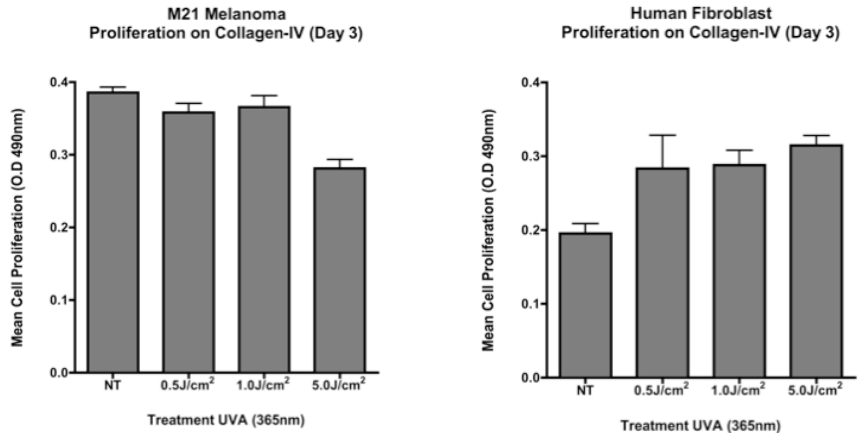

Figure 4. UVA-irradiation of collagen type-IV alters M21 melanoma and fibroblast cell proliferation in vitro. Collagen type-IV was either not treated or irradiated with UVA (365nm) over a dose range (0-5.0J/cm^2). Microtiter wells were coated (5.0ug/ml) with untreated or UVA treated collagen and M21 melanoma cells (A) and human dermal fibroblasts (B) were seeded in wells and allowed to grow over a 3-day time course. Proliferation was monitored using MTT assay. Data bars represent mean proliferation (Optical Density O.D) $\pm$ standard deviations from triplicate wells.

Exposure of the HU177 cryptic epitope within Matrigel^{TM} in vitro. To begin to assess whether specific UV wavebands my trigger exposure of the HU177 epitopes within Matrigel^{TM}, a secreted basement membrane-like ECM composed predominately of laminin and collagen type-IV, we irradiated Matrigel^{TM} with UVB over a dose range (0-5J/cm^2). Solid phase ELISA assays were carried out to assess the relative exposure of the HU177 epitope. Surprising, the HU177 epitope could be detected in non-irradiated Matrigel^{TM} (Figure 5). Interestingly, while a small enhancement of reactivity could be detected following UVB irradiation at a dose of 0.5J/cm^2, a dose of 5.0J/cm^2 reduced reactivity with anti-HU177 antibody. These data suggest that the HU177 cryptic collagen epitope appears to be exposed within Matrigel^{TM} prior to UV-irradiation and that collagen type-IV present within Matrigel^{TM} is at least partially in a non-triple helical conformation.

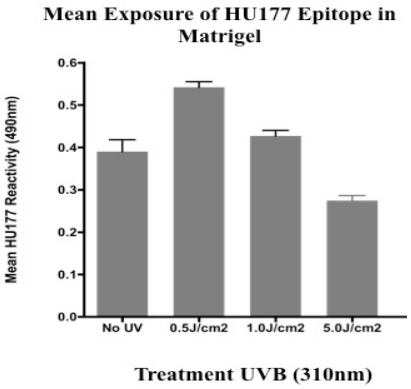

Figure 5. UV-mediated exposure of the HU177 cryptic collagen epitope within Matrigel^{TM} in vitro. Matrigel^{TM} was untreated or irradiated with UVB over the dose range indicated and coated on microtiter wells. Exposure of the HU177 cryptic epitope was detected by solid phase ELISA. Data bars represent the mean Mab D93 reactivity (Optical Density O.D) $\pm$ standard deviations from triplicate wells.

Differential adhesion of human M21 melanoma cells and dermal fibroblasts to UVB-irradiated Matrigel^{TM}. Given our previous studies suggesting differentially enhanced melanoma cell adhesion to UV-irradiated collagen I and IV, we examined the effects of UV-irradiation on cell adhesion to basement membrane preparation Matrigel^{TM}. Matrigel^{TM} was irradiated with UVB over a dose range from 0-5.0J/cm^2. Surprisingly, as shown in figure 6A, human M21 melanoma cell adhesion to UVB-irradiated Matrigel^{TM} was

inhibited by nearly 40% at 5.0J/cm^2. In contrast, dermal fibroblast adhesion was enhanced dose dependently, exhibiting a maximum enhancement at a UVB dose of 1.0J/cm^2 (figure 6B).

A. **B.**

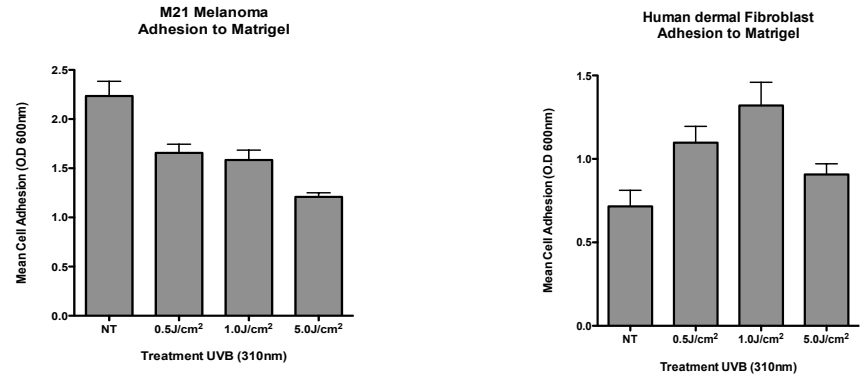

Figure 6. Alterations of melanoma cell interactions with UV-irradiated Matrigel™. Non-treated and irradiated Matrigel™ were coated on wells and blocked with BSA in PBS. A). M21 melanoma cells or B) human dermal fibroblasts were seeded on the wells and allowed to attach as we previously described (1-3). Data bars represent mean cell adhesion (Optical Density O.D) ± standard deviations from triplicate wells.

Differential adhesion of human M21 melanoma cells and dermal fibroblasts to UVA-irradiated Matrigel™. Given the differential impact of UVB-irradiated Matrigel™ had on cell adhesion, we examined the effects of UVA-irradiation on cell adhesion to Matrigel™ using a similar assay. Matrigel™ was irradiated with UVA over a dose range from 0-5.0J/cm^2. Surprisingly, in contrast to UVB (figure 6A), M21 melanoma cell adhesion to UVA-irradiated Matrigel™ was enhanced by greater than 50% at 0.5J/cm^2 or higher as compared to control. In addition, human dermal fibroblast adhesion was enhanced by nearly 40%, at a UVA dose of 5.0J/cm^2 (figure 7B). These important studies indicate the complex and potentially opposing effects of UVA as compared to UVB on cell adhesive behavior.

A. **B.**

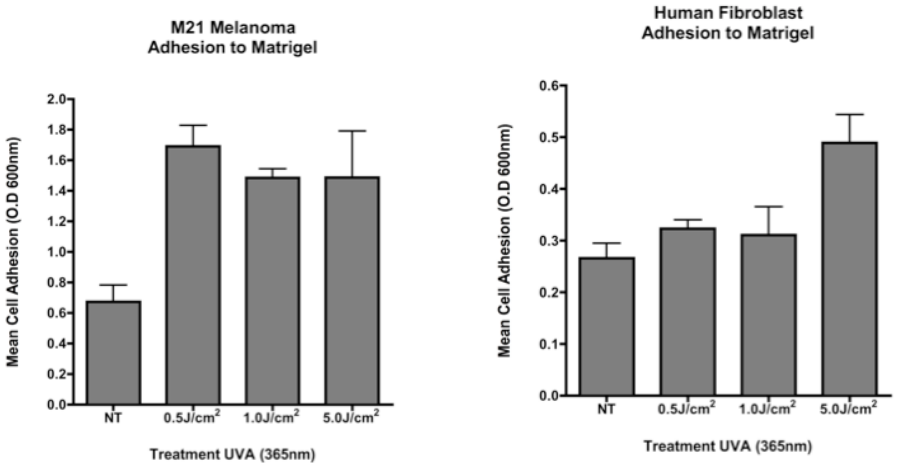

Figure 7. Alterations of melanoma cell interactions with UVA-irradiated Matrigel™. Non-treated and irradiated Matrigel™ were coated (5.0ug/ml) on wells and blocked with BSA. A). M21 melanoma cells or B) human fibroblasts were seeded on the wells and allowed to attach as we previously described (1-3). Data bars represent mean cell adhesion (Optical Density O.D) ± standard deviations from triplicate wells.

UVA-irradiation of Matrigel™ differentially alters human melanoma and fibroblast proliferation in vitro. To assess the effects of UVA irradiated Matrigel™ on melanoma and fibroblast growth in vitro, we carried out in vitro proliferation assays. Briefly, Matrigel™ was either untreated or irradiated with UVA over a dose range (0-5.0 J/cm^2) and proliferation was assessed over a time course (0-72hrs). Little change in the proliferation of either M21 melanoma or fibroblasts was observed under the experimental conditions within the first 48hrs. However, as shown in figure 8A, a small reduction was observed in M21 melanoma cell growth on UVA irradiated Matrigel™ as compared to control by day 3. In contrast, an approximately 50% increase in fibroblast growth was observed by day 3 at a dose of 0.5J/cm^2 or higher (figure 8B).

A. **B.**

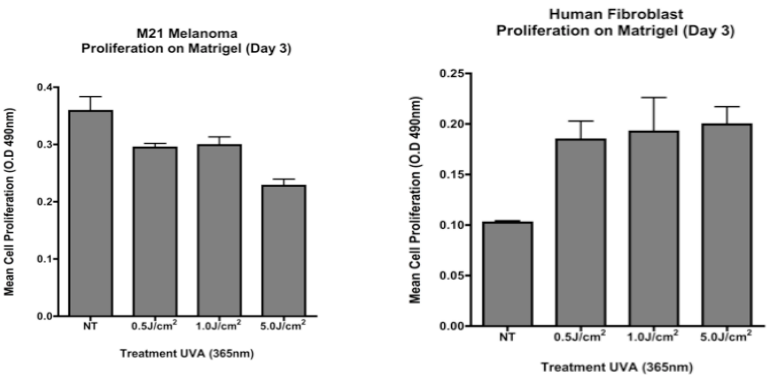

Figure 8. UVA-irradiation of Matrigel™ alters M21 melanoma and fibroblast proliferation in vitro. Matrigel™ was either not treated or irradiated with UVA (365nm) over a dose range (0-5.0J/cm^2). Microtiter wells were coated (5.0ug/ml) with untreated or UVA treated Matrigel™ and M21 melanoma cells (A) and dermal fibroblasts (B) were seeded in wells and allowed to grow over a 3-day time course. Cell proliferation was monitored using MTT assay. Data bars represent mean cell proliferation (Optical Density O.D) ± standard deviations from triplicate wells.

Differential migration of M21 melanoma cells and Raw 264.7 macrophages on UV-irradiated Matrigel™. Given our previous studies, we examined the effects of UV-irradiation on cell migration on Matrigel™. Matrigel™ was irradiated with UVB over a dose range from 0-5.0J/cm^2 and M21 melanoma cells or Raw 264.7 macrophages were allowed to migrate using Matrigel™ coated transwell migration chambers. As shown in figure 9A, enhanced migration of M21 melanoma cells was detected on Matrigel™ irradiated at a dose of 0.5J/cm^2, while little change was detected in migration on Matrigel™ irradiated at higher doses. In contrast, reduced macrophage migration was observed on Matrigel™ irradiated with increasing doses of UVB (figure 9B). These data again confirm the complex cell type and dose-dependent changes in cellular behavior that occur as a result of UV-mediated structural alteration of ECM proteins in vitro.

A. **B.**

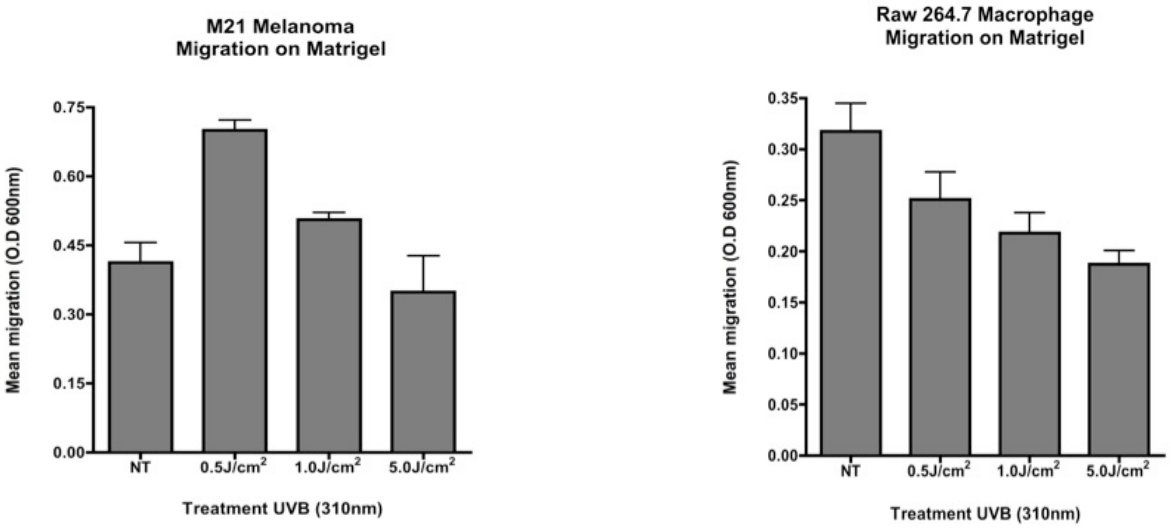

Figure 9. Differential migration of M21 melanoma cells and Raw 264.7 macrophages on UV-irradiated Matrigel™. Non-treated and irradiated Matrigel™ (5.0ug/ml) were coated on membranes of transwell migration chambers. Sub-confluent cells were resuspended in migration buffer and seeded in the upper chamber. A). Quantification of M21 melanoma cells migration. B) Quantification of Raw 264.7 macrophage migration. Data bars represent mean cell migration (Optical Density O.D) ± standard deviations from triplicate wells.

UVB-irradiation of Matrigel™ fails to alter M21 melanoma cell proliferation in vitro. To assess the effects of UVB irradiation of Matrigel™ on melanoma cell growth in vitro, we carried out in vitro proliferation assays. Briefly, Matrigel™ was either untreated or irradiated with UVB over a dose range (0-5.0 J/cm^2) and proliferation was assessed over a time course (0-72hrs). As shown in figure 10A-C, UVB irradiation of Matrigel™ failed to significantly alter M21 melanoma cell proliferation over the time course tested. These findings suggest that while UVB irradiation of Matrigel™ alters melanoma cell adhesion, it caused little if any change on their ability to grow over the 3-day time course.

A. **B.** **C.**

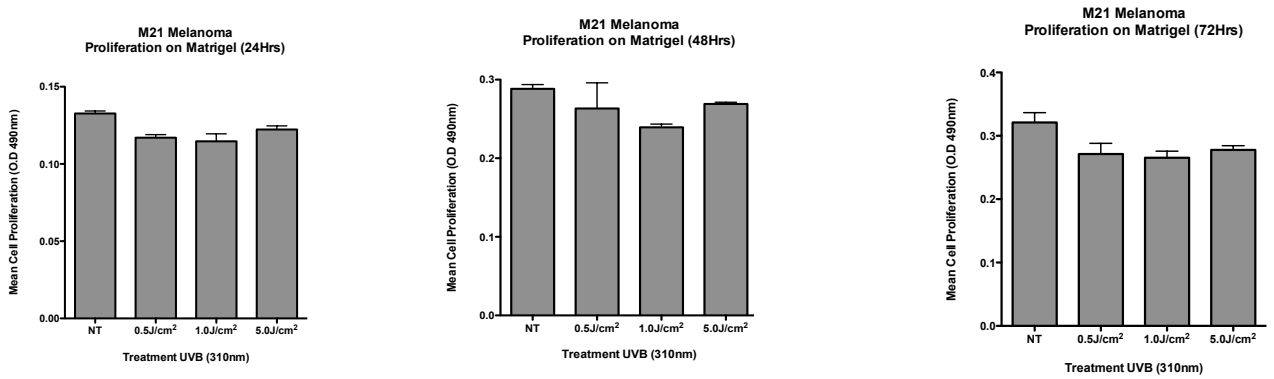

Figure 10. UVB-irradiation of Matrigel™ fails to alter M21 melanoma cell proliferation in vitro. Matrigel™ was either not treated or irradiated with UVB (310nm) over a dose range (0-5.0J/cm^2). Microtiter wells were coated (5.0ug/ml) with untreated or UVB treated Matrigel™ and M21 melanoma cells were seeded in wells and allowed to grow over a 3-day time course. Tumor cell proliferation was monitored using MTT assay. Data bars represent mean cell proliferation (Optical Density O.D) $\pm$ standard deviations from triplicate wells.

UVB-irradiation of collagen type-IV enhances murine macrophage migration. Our previous studies suggested that UVB-irradiation of collagen type-IV, but not collagen type-1 could enhance macrophage adhesion. These findings are consistent with the possibility that UVB irradiation induces a structural change in collagen type-IV that facilitates enhanced adhesion. In this regard, we examined whether UVB-mediated structural change in collagen type-IV could also enhance macrophage migration. To examine this possibility, Raw 264.7 macrophages were allowed to migrate on transwells coated with either untreated or UVB-treated (5.0J/cm^2) collagen type-I or collagen type-IV. As shown in figure 11A, macrophages exhibited similar migratory capacity on either untreated or UVB-irradiated collagen type-I. In contrast, macrophage exhibited enhanced migration on UVB-irradiated collagen type-IV as compared to untreated collagen type-IV (figure 11B). These data are consistent with our previously reported adhesion data and suggest that a unique UVB-mediated structural change in collagen type-IV, but not collagen type-I enhances macrophage migration.

A **B.**

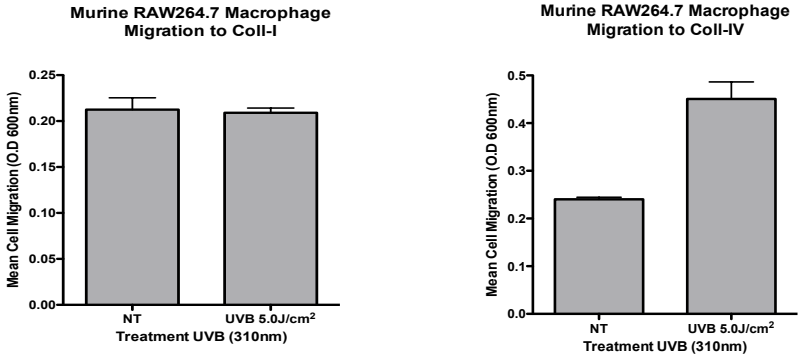

Figure 11. Alterations of macrophage interactions with UV-irradiated collagen-IV Non-treated and UVB irradiated (5.0J/cm^2) collagen type-I (A) and collagen type-IV (B) were coated (5.0ug/ml) on membranes of transwell migration chambers. RAW 264.7 macrophages were seeded and allowed to migrate as we described (1-3). Data bars represent mean cell migration (Optical Density O.D) $\pm$ standard deviations from triplicate wells.

UVB-irradiation of collagen type-IV enhances macrophage proliferation in vitro. Given the consistent findings indicating that UVB-mediated structural change in collagen type-IV alters the adhesive and migratory

behavior of macrophages on this ECM substrate, we assessed the effects of UVB irradiation of collagen type-IV on macrophage growth in vitro. Briefly, collagen type-IV was either untreated or irradiated with UVB (5.0 J/cm^2) and proliferation was assessed over a time course (0-72hrs). As shown in figure 12A-C, UVB irradiation of collagen type-IV enhanced proliferation by approximately 30% to 40% over the time course tested. These findings are consistent with UVB-mediated structural change in collagen type-IV altering the behavior of macrophages in vitro.

A. **B.** **C.**

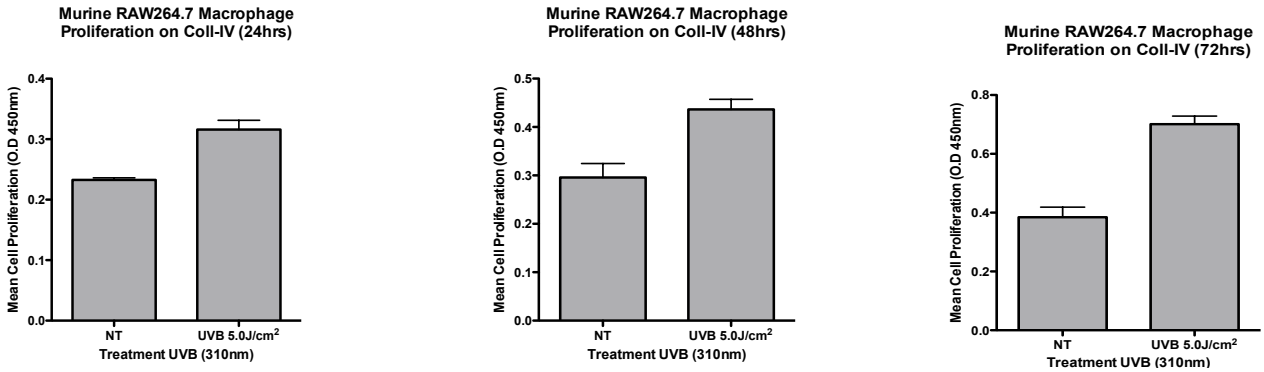

Figure 12. UVB-irradiation of collagen type-IV alters macrophage proliferation in vitro. Collagen type-IV was either not treated or irradiated (0-5.0J/cm^2) with UVB (310nm). Microtiter wells were coated (5.0.0ug/ml) with untreated or UVB treated collagen and murine macrophages were seeded in wells and allowed to grow over a 3-day time course. Proliferation was monitored using MTT assay. Data bars represent mean cell proliferation (Optical Density O.D) $\pm$ standard deviations from triplicate wells.

UV-mediated induction of inflammatory cells in mouse skin. To begin to establish a time course and dose of UV irradiation needed to induce a reproducible inflammatory response in full thickness mouse skin, mice were irradiated with UVB over a dose range of 0-1.0J/cm^2 and skin has harvested 24hrs, 48hrs and 72hrs later. The full thickness skin was either snap frozen or embedded in paraffin and tissues sections prepared. To examine the tissues for inflammatory infiltrates the tissues were stained by Giemsa. As shown in figure 13A middle panel, UVB at a dose of 0.1J/cm^2 induced infiltration of inflammatory cells (arrows) primarily confined to the subcutaneous fat with minor infiltration into the lower regions of the dermis by 24 hours as compared to non-UV (left panel). UVB irradiation with a dose of 1.0Jcm^2 (right panel) induced a strong inflammatory infiltrate into the middle and upper levels of the dermis (Rights panel). Little over all changes could be detected in the relative levels inflammatory infiltrates between 48 and 72 hours following UV irradiation (figure 13B an C). Under these conditions, our data suggests that UVB irradiation at either 0.1Jcm^2 or 1.0Jcm^2 induces a significant inflammatory infiltrate.

A.

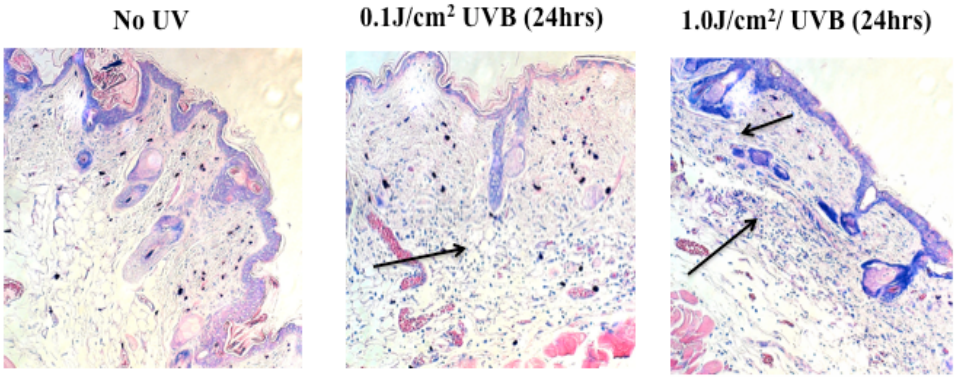

B.

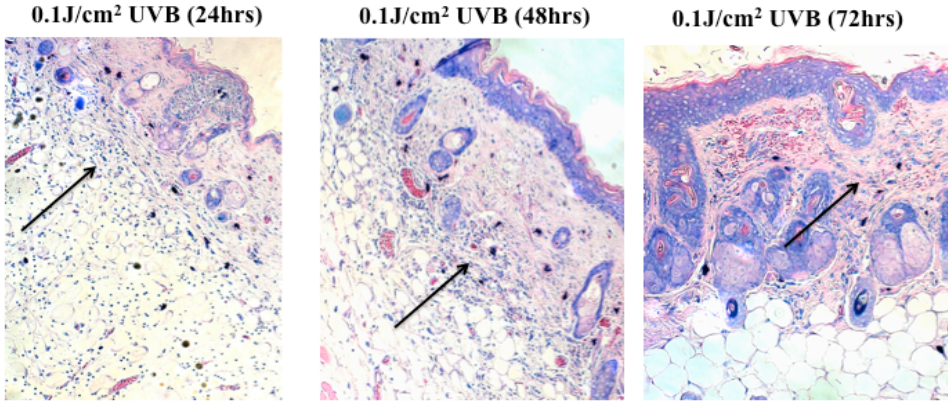

C.

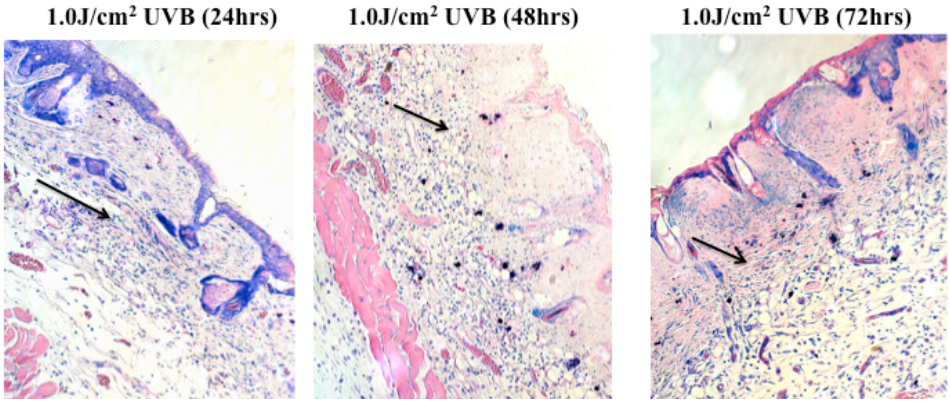

Figure 13. UV-mediated induction of inflammatory cells in mouse skin. Mice (nude) were either not treated or irradiated (0.1-1.0J/cm^2) with UVB (310nm). Mice were sacrificed over a time course of 3 days (24hrs, 48hrs or 72hrs) and full thickness skin was harvested and embedded in paraffin. Tissue sections were cut and stained by Giemsa method to detect immune cells (arrows). Small blue cells include neutrophils, larger cells with characteristic large nuclei include macrophages, and dark purple granulated cells include mast cells. A). Representative examples of mouse skin from either untreated left panel (No UV) or UVB-irradiated middle panel (UVB 0.1J/cm^2), or right panel (UVB 1.0J/cm^2). B). Representative examples of mouse skin from UVB- irradiated (0.1J/cm^2) left panel (24hrs) or middle panel (48hrs), or right panel (72hrs). C). Representative examples of mouse skin from UVB- irradiated (1.0J/cm^2) left panel (24hrs) or middle panel (48hrs), or right panel (72hrs). Black arrows indicate examples of immune infiltrates. All photos taken at a magnification of 100x.

Immunofluorescence detection of elevated neutrophils in UVB-irradiated mouse skin. Given our studies establishing the parameters useful for inducing UV-mediated inflammatory cell infiltration into full thickness mouse skin, we began to characterize the types of inflammatory cell infiltrates that were induced by UV-irradiation in this mouse model. Frozen sections of full thickness murine skin from either untreated or UVB irradiated were analyzed for the presence of neutrophils using the previously described murine neutrophil marker (7/4 antigen). As shown in figure 14, few neutrophils could be detected with the epidermis or dermis of non-irradiated skin (left panels). In contrast, 24hrs post UVB irradiation (top panels) a dose dependent increase in neutrophil infiltration (red) could be readily detected. Importantly, 48hrs post UV irradiation, neutrophils persisted following UV-irradiation at 1.0Jcm^2. These data confirm a time and dose dependent infiltration of neutrophils following UVB-irradiation.

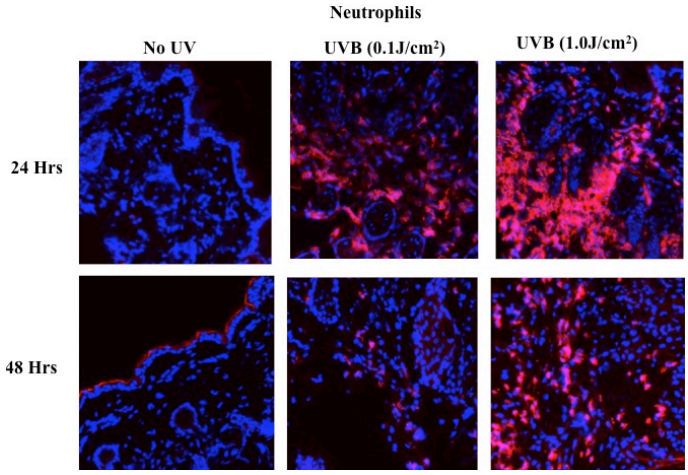

Figure 14. Detection of elevated levels of neutrophils in UVB-irradiated mouse skin. Mice (nude) were either not treated or irradiated (0.1-1.0J/cm^2) with UVB (310nm). Mice were sacrificed at 24hr and 48hrs and full thickness skin was harvested and embedded. Tissue sections were cut and stained for the presence of infiltrating neutrophils. Red color indicates neutrophils (7/4 antigen) and blue indicated Dapi. All photos taken at a magnification of 200x.

Immunofluorescence detection of macrophages in UVB-irradiated mouse skin. Given our studies suggesting elevated neutrophil infiltration following UVB-irradiation, we examine murine skin for the presence of macrophages. In contrast to neutrophils, macrophages could be detected in normal non-irradiated skin and by 48hrs post UV-irradiation some enhancement of the relative levels of macrophages could be detected at 1.0J/cm^2, however little change was detected at lower doses of UVB-irradiation or at earlier time points (Figure 15). These data, in conjunction with the distinct enhancement of mast cell infiltration (see figure 13, purple granulated cells following Giemsa staining) confirm the differential induction of distinct subsets of inflammatory cells following UVB-irradiation of murine skin.

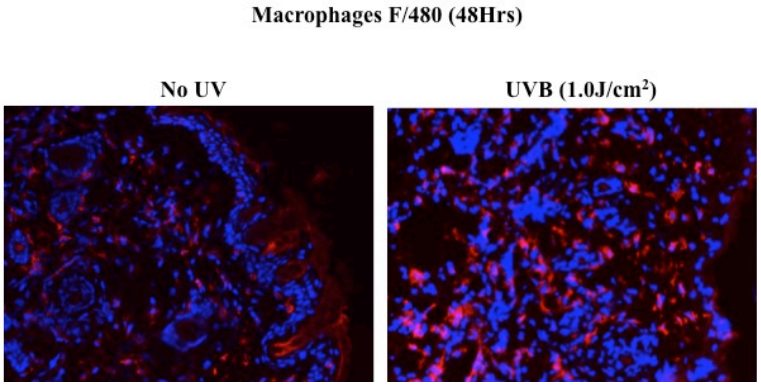

Figure 15. Detection of elevated levels of macrophages in UVB-irradiated mouse skin. Mice (nudes) were either not treated or irradiated (0.1-1.0J/cm^2) with UVB (310nm). Mice were sacrificed at 48hrs and full thickness skin was harvested and embedded. Tissue sections were cut and stained for the presence of macrophages (F4/80 antigen). Red color indicates macrophages and blue indicated Dapi. All photos taken at a magnification of 200x.

Immunofluorescence detection of altered proteolytic enzymes in UVB-irradiated mouse skin. Previous studies have implicated enhanced expression of a number of proteolytic enzymes in activated neutrophils and macrophages (4-6). Our previous studies have suggested that enzymes such as MMPs may contribute to the exposure of cryptic collagen epitopes in vivo (2). Therefore, we began to examine the expression of enzymes known to be expressed by inflammatory infiltrates including the serine protease neutrophil elastase and the gelatinase MMP-9. As shown in figure 16A, coinciding with the elevated infiltration of neutrophils, enhanced levels of neutrophil elastase could be readily detected predominately within the epidermal and dermal layers by 48hrs following UVB-irradiation (1.0J/cm^2). In similar studies, elevated levels of MMP-9 were also detected with strong staining noted in the epidermis and surrounding dermal blood vessels and scattered dermal cells (Figure 16B). These data confirm enhanced levels of proteolytic enzymes, which might contribute to the exposure of the HU177 epitope in vivo following UVB irradiation.

A. **B.**

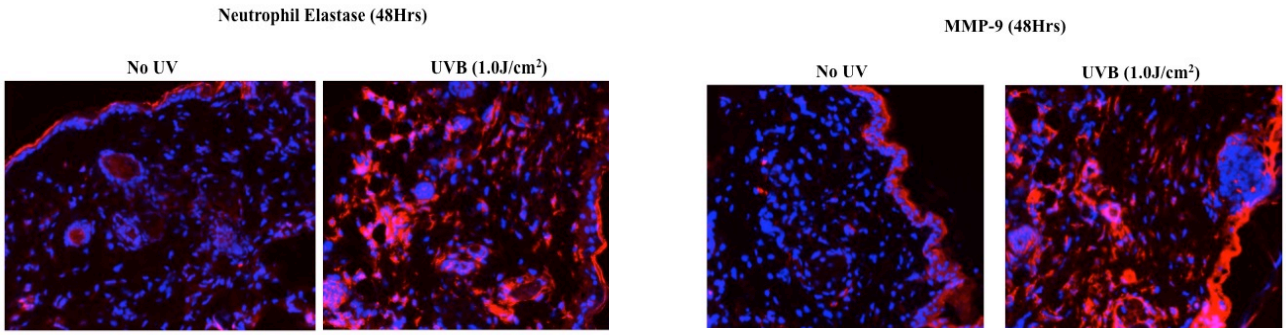

Figure 16. Detection of altered proteolytic enzymes in UVB-irradiated mouse skin. Mice (nude) were either not treated or irradiated (0.1-1.0J/cm^2) with UVB (310nm). Mice were sacrificed at 48hrs and full thickness skin was harvested and embedded. Tissue sections were cut and stained for the presence of Neutrophil Elastase or MMP-9. A). Red color indicates Neutrophil Elastase and Blue indicated Dapi. B). Red color indicates MMP-9 and Blue indicated Dapi All photos taken at a magnification of 200x.

Blocking the HU177 cryptic collagen epitope inhibits UVB-induced mast cell accumulation in skin. Given our studies establishing the experimental parameters useful for inducing UV-mediated inflammatory cell infiltration into full thickness mouse skin, we began to examine the effects of blocking cellular interactions with the HU177 cryptic collagen epitope on UV-mediated mast cell accumulation within skin. Briefly, mice were either untreated or injected with a single i.p injection (100ug/mouse) of function blocking anti-HU177 humanized Mab D93 or non-specific control IgG. Twenty-four hours later mice were either not irradiated or irradiated with UVB (0.1J.cm^2) and full thickness skin was harvested 24hrs later. Tissue sections were prepared as described above and mast cell (dark purple granulated cells) infiltration into the dermis was evaluated following Giemsa staining. Importantly, examination of the tissue sections from each experimental condition suggested a reduction in the relative levels of mast cell accumulation within the dermal regions of the skin of mice pretreated with anti-HU177 humanized Mab D93 as compared to controls (figure 17A). In fact, quantification of the relative levels of mast cells per 200X field indicated a near complete inhibition of UV-induced mast cell accumulation back to levels prior to UVB irradiation, while a non-specific control antibody exhibited minimal change (figure17B). These exciting new data suggest that the HU177 epitope may play a functional role in UVB-induced mast cell accumulation in the skin.

A. **B.**

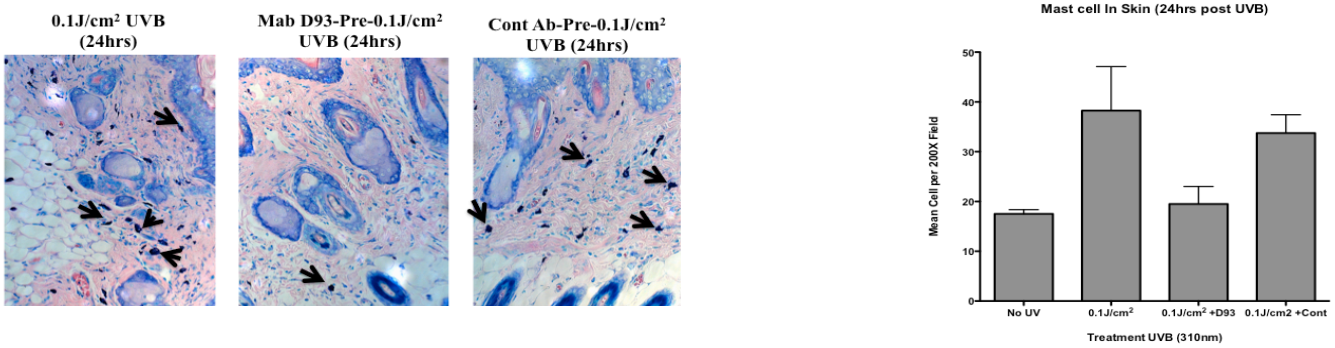

Figure 17. Anti-HU177 Mab inhibits UVB-mediated mast cell accumulation in skin. Mice (nude N=4) were not treated or treated with a single i.p injection of D93 Mab or control (100ug). Twenty-four hours later mice were not irradiated or irradiated (0.1J/cm^2) with UVB. Mice were sacrificed 24hrs later and skin was embedded in paraffin. Tissue sections were cut and stained by Giemsa to detect mast cells (arrows heads). A). Representative examples of mouse skin from UVB 0.1J/cm^2 irradiated (left panel) or pre-treated with Mab D93 and UVB-irradiated (middle panel) or pre-treated with control Ab and UVB-irradiated (Right panel). Dark purple granulated cells at arrows show examples of mast cells. B) Quantification of the mean number of mast cells within the dermal region of the skin. Data bars represent the mean mast cells per 200X field $\pm$ Standard Error from 10 independent fields.

UVB irradiation-induced enhancement of melanoma growth depends in part on the HU177 epitope. Given our studies indicating that 0.1J/cm^2 can induced a strong infiltration of inflammatory cells including neutrophils, mast cells and macrophages and these cell types have been suggested to contribute to tumor initiation and growth (7-10), we examined the impact of UVB-irradiation on M21 melanoma growth in nude mice. Briefly, mice were either untreated or pre-treated with a single i.p injection of 100ug of anti-HU177 epitope antibody D93. Twenty-four hours later mice were not irradiated or irradiated with a single dose of UVB (310) 0.1J/cm^2. Twenty-four hours later mice were injected subcutaneously with M21 melanoma cells (3x10^6). Melanoma tumor growth was monitored over a time course of 21 days. As shown in figure 18A, a single UVB dose of irradiation resulted in larger tumors as compared to control (NT). Importantly, pretreating the mice prior to UVB-irradiation resulted in smaller tumors as compared to UVB–irradiated mice. In fact, quantification of tumor size indicated that pre-treating mice with a single 100ug injection of anti-HU177 cryptic epitope antibody prior to UVB –irradiation inhibited melanoma tumor growth by nearly 40% as compared to control (figure 18B). These preliminary experiments suggest that UVB-irradiation enhancement of melanoma growth in these mice may be do in part, to the functional exposure of the HU177 cryptic collagen epitope.

A. **B.**

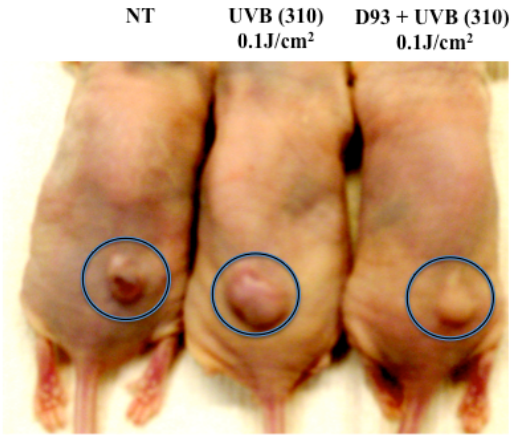

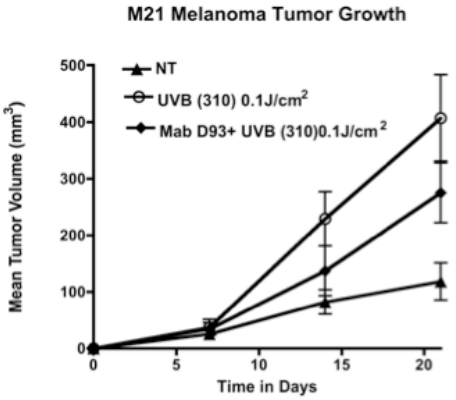

Figure 18. UVB Irradiation-induced enhanced M21 melanoma growth depends in part on the HU177 epitope. Mice (N=5-7) were not treated or injected with a single i.p treatment with anti-HU177 humanized antibody D93 (100ug). Twenty-four hours later mice were not irradiated or irradiated (0.1J/cm^2) with UVB (310nm). Twenty-four hours later, mice were injected subcutaneously with M21 melanoma cells (3x10^6). Mice were sacrificed at day 21. Tumor growth was monitored by caliper measurements. A). Representative examples of mice from either non-treated controls (left panel), UVB 0.1J/cm^2 irradiated (middle panel) or pre-treated with Mab D93 and UVB-irradiated (right panel). B) Quantification of the mean tumor volume from each experimental condition. Data bars represent the mean tumor volume $\pm$ Standard Error.

Exposure of the HU177 cryptic epitope in full thickness human skin following ex vivo UV-irradiation. Our previous studies have indicated the UV-irradiation of purified collagen in vitro can result in structural changes that lead to exposure of the HU177 epitope. To begin to characterize the human neonatal foreskin that will be used in the human/mouse chimeric model, we first assessed whether UV-irradiation can also expose the HU177 epitope in full thickness human skin. Briefly, surgical explants of discarded neonatal human foreskin was either not treated or irradiated with UVA and UVB ex vivo at either 0.1J/cm^2 or 1.0J/cm^2. Tissues were either snap frozen or embedded in paraffin and tissues section prepared. To assess basal levels of any inflammatory cells within these human skin samples following surgical resection, tissues were stained by Giemsa. As shown in figure 19A, UV-irradiation of explanted full thickness human skin exhibited few if any inflammatory infiltrates and were similar to untreated control skin since these human skin samples were surgically removed from patients prior to UV-irradiation. The relative levels and distribution of collagen within both non-treated and UV-irradiated human skin were also similar as indicated by trichrome staining (figure 19B). Importantly, while some exposure of the HU177 epitope was detected in these untreated skin

specimens, UV-irradiation of these surgically explanted full thickness human skin samples resulted an enhanced exposure of the HU177 cryptic collagen epitope primarily within the dermal region with some minor exposure detected in the epidermal regions (figure 19C). These studies suggest that while inflammatory infiltrates may contribute to and enhance the exposure of the HU177 epitope, UV-irradiation may expose the HU177 epitope within full thickness human skin in the absence of elevated levels of inflammatory infiltrates.

A.

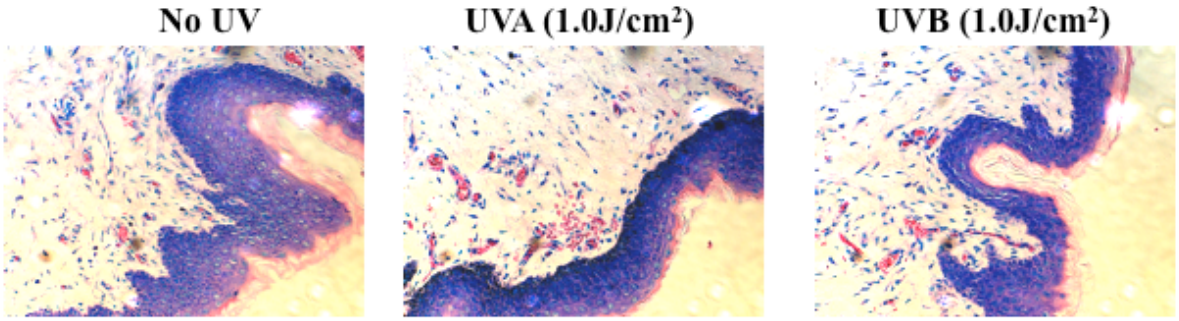

B.

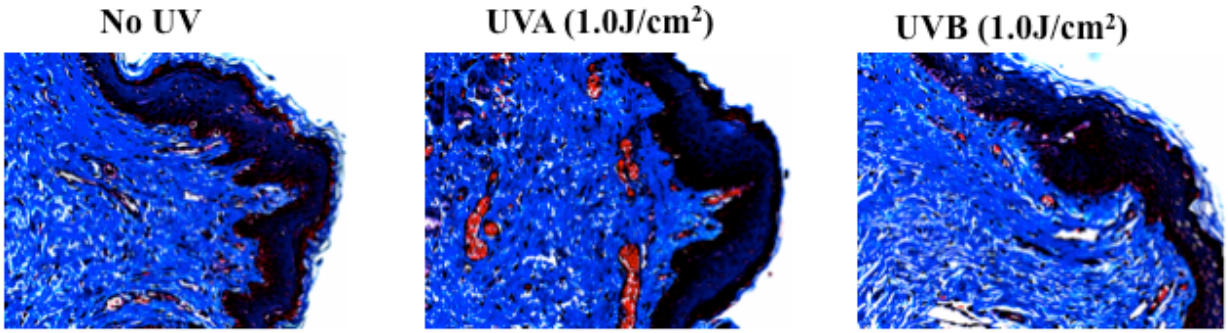

C.

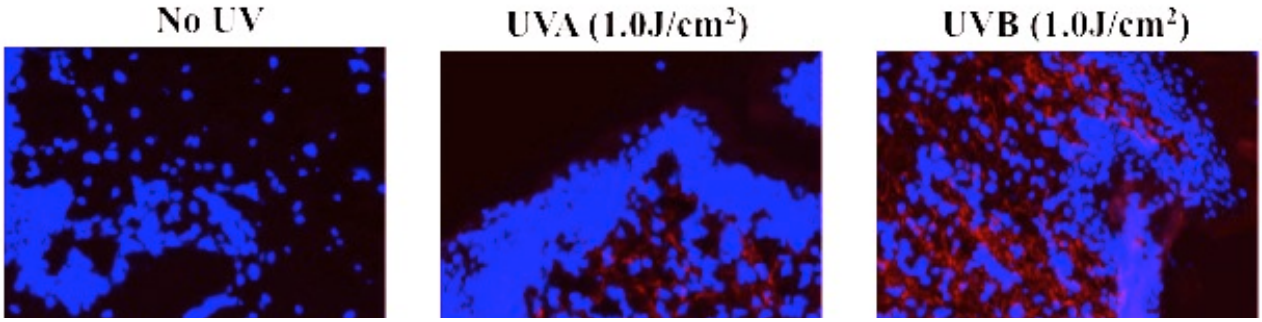

Figure 19. Detection of enhanced exposure of the HU177 epitope in ex-vivo UV-irradiated human skin. Fresh human neonatal foreskin obtained 24hrs following surgical resection was either not treated or irradiated ex vivo (1.0J/cm^2) with UVA (365nm) or UVB (310nm). Full thickness human skin was embedded and tissues sections prepared. Tissues stained by Giemsa (A), Trichrome (B) or with anti-HU177 Mab (C). A). Representative examples of human skin stained by Giemsa. B). Representative examples of human skin stained by Trichrome with blue color indicating collagen. C). Representative examples of human skin stained for exposure of the HU177 collagen epitope with Red color indicating exposure of the HU177 epitope. All photos taken at a magnification of 200x.

Key Research Accomplishments:

1). UVA and UVB irradiation of ECM proteins alter the adhesive behavior of fibroblast, melanoma cells and macrophages in vitro.

2). UVA and UVB irradiation of ECM proteins alter the migratory behavior of fibroblast, melanoma cells and macrophages in vitro.

3). UVA and UVB irradiation of ECM proteins alter the proliferative behavior of fibroblast, melanoma cells and macrophages in vitro.

4). UVB-irradiation of mouse skin induces inflammation in a dose and time dependent manner.

5). UVB-irradiation of mouse skin induces enhanced levels of neutrophil elastase and MMP-9 in a dose and time dependent manner.

6). UVB-induced accumulation of mast cells in the skin depends in part on the HU177 collagen epitope.

7). UVB-irradiation of muse skin enhances the growth of M21 melanoma in vivo.

8). UVB-enhanced growth of M21 melanoma tumors in vivo, depend in part on the HU177 collagen epitope.

9). UV-irradiation of full thickness human skin explants results in exposure of the HU177 epitope.

Reportable Outcomes: None

Conclusions:

Our current experimental findings indicate that irradiation with UVA and UVB wavebands results in unique structural changes in collagen type-I, and collagen type-IV in vitro, leading to the exposure of the HU177 cryptic collagen epitope. Surprisingly, the conformation of collagen type-IV present within the commercially obtained ECM preparation Matrigel^{TM} is at lease partly denatured as the HU177 cryptic epitope was detected prior to expose to UV–irradiation. Interestingly, a dose dependent increases in UV-irradiation caused a reduction in reactivity with anti-HU177 antibody, suggesting that differential UV-mediated alterations in the structure of the Matrigel^{TM} can disrupt functional exposure of the HU177 epitope. In addition, our current studies suggest that UV-mediated structural alterations in both collagen type-I and collagen type-IV differentially alter the ability of human melanoma cells, human dermal fibroblasts and macrophages to attach, migrate and proliferate on these substrates in vitro. Importantly, these changes in cellular behaviors largely depended on the cell type, waveband, dose of irradiation and type of ECM examined. These in vitro results are consistent with the ability of UV-irradiation of ECM proteins to differentially alter the response of distinct subsets of tumor and normal stromal cells to ECM proteins that help make up the epidermal and dermal regions of the skin.

Our current in vivo studies have indicated that UVB irradiation of murine skin at a dose of at least 0.1Jcm^2 can induce a rapid infiltration of inflammatory cells into the subcutaneous fat underlying the skin with some infiltration into the lower dermal regions by 24hrs. Between 48 hours and 72 hours the inflammatory cells were more widely detected throughout the dermis and in some cases observed in the epidermal region suggesting a rapid and time dependent inflammatory response with the doses of UVB tested. Distinct subsets of inflammatory cells were identified including an early infiltration of neutrophils and mast cells that were only minimally detected in non-irradiated skin. In contrast, macrophages were abundantly detected in normal non-irradiated skin and increased levels were only detected at higher doses of UVB seen at post treatment times of at least 48 hours indicating a clear differential kinetic response of specific subsets of inflammatory cells following UV-irradiation. Moreover, specific enhancement in the levels of the serine protease neutrophil

elastase and the matrix metalloproteinase-9 (MMP-9) were detected within 48hrs of UVB irradiation, indicating elevated levels of inflammation associated enzymes that may contribute to the exposure of the HU177 cryptic collagen epitope within the skin.

With the experimental parameters established for UV-irradiation of full thickness skin, we examined the possible role of the HU177 cryptic collagen epitope to regulate UV-mediated infiltration of inflammatory cells. Given the differential impact of UV-radiation treated collagen on distinct subset of cells, we first assessed the effects of function blocking antibodies on mast cells. Our data indicate that a single injection (100ug/mouse) significantly ($P<0.05$) inhibited UVB-induced accumulation of mast cells suggesting a function role for the HU177 epitope in this process. Given the possible role of inflammatory cells in helping to create a tumor permissive microenvironment, we examined the effects of UVB on tumor growth. Our data indicate that a single UVB dose of 0.1J/cm to the mouse skin given 24hrs prior to melanoma cell inoculation resulted in the formation of melanoma tumors that were nearly 4 fold larger than those that formed in non-irradiated mice. Moreover, pre-treating the mice with a single (100ug/mouse) dose of Mab D93 reduced the UV-associated increase in tumor growth by nearly 40%, suggesting a possible functional role the HU177 epitope in UV-enhanced tumor growth. Taken together, we have made substantial progress in the overall goals of our proposal as indicated by the initiation and progress with specific aim 1, tasks 1-3, specific aim 2 tasks 1-3 and specific aim 3 tasks 1 and 2. In conclusion, our current findings suggest that not only can UV-irradiation of specific ECM proteins alter the behavior of both stromal and tumor cells on specific ECM substrates in vitro, but that UV-radiation associated accumulation of mast cells in the skin and UVB-enhanced melanoma tumor growth may depend in part on the functional exposure of the HU177 collagen epitope in vivo.

References:

1). Xu, J. Rodriguez, D., Petitclerc, E., Kim, J. J., Hangai, M., Moon, Y. S., Davis, G. E., and Brooks, P. C. Proteolytic exposure of a cryptic site within collagen type-IV is required for angiogenesis and tumor growth. J. Cell Biol. 154: 1069-1079. 2001.

2). Hangia, M., Kitaya, N., Xu, J., Chan, C. K., Kim, J. J., Werb, Z., Ryan, S. J., and Brooks, P. C. Matrix metalloproteinase-9-dependent exposure of a cryptic migratory control site in collagen is required before retinal angiogenesis. Am. J. Pathol. 161: 1439-1437. 2002.

3). Petitclerc, E., Stromblad, S., von Schalscha, T. L., Mitjans, F., Piulats, J., Montgomery, A. M., Cheresh, D. A., and Brooks, P. C. Integrin $\alpha v\beta 3$ promotes M21 melanoma growth in human skin by regulating tumor cell survival. Cancer Res. 59: 2724-2730. 1999.

4). Takeuchi, H., Gomi, T., Shido, M., Watanabe, H., and Suenobu, N. Neutrophil elastase contributes to extracellular matrix damage induced by chronic low-dose UV irradiation in hairless mouse photoaging model. J. Dermatol. Sci. 60: 151-158. 2010.

5). Heissig, B., Nishida, C., Tashiro, Y., Sato, Y., Ishihara, M., Ohki, M., Gritli, I., Rosenkvist, J., and Hattori, K. Role of neutrophil-derived matrix metalloproteinase-9 in tissue regeneration. Histol. Histopathol. 25: 765-770. 2010.

6). Pittoni, P., and Colombo, M. P. The dark side of mast cell-targeted therapy in prostate cancer. Cancer res. 72: 831-835. 2012.

7). Schreiber, R. D., Old, L. J., and Smyth, M. J. Cancer immunoediting: intergrating immunity's role in cancer suppression and promotion. Science. 331: 1565-1570. 2011.

8). Heusinkveld, M., van der Burg, S. H. Identification and manipulation of tumor-associated macrophages in human cancers. J. Transal. Med. 9: 216-228. 2011.

9). Chow, M. T., Moller, A., and Smyth, M. J. Inflammation and immune surveillance in cancer. Semin. Cancer Biol. 22: 23-32. 2012.

10). Bronkhorst, I H., Ly, L. V., Jordanova, E. S., Vroliijk, J., Versluis, M., Luyten, G. P., and Jager, M. J. Detection of M2-macrophages in uveal melanoma and relation with survival. Invest. Ophthalmol. Vis. Sci. 52: 643-650. 2011.

Appendices: none